

Article

Transfer Learning On Small Datasets for Improved Fall Detection

Nader Maray¹, Anne H.H. Ngu^{1*}, Jianyuan Ni¹, Minakshi Debnath¹, and Lu Wang¹

¹ Department of Computer Science, Texas State University, San Marcos, Texas, 78666

Academic Editor: name

Version February 1, 2023 submitted to Sensors; Typeset by L^AT_EX using class file mdpi.cls

Abstract: Falls in the elderly are associated with significant morbidity and mortality. While numerous fall detection devices incorporating AI and machine learning algorithms have been developed, no known smartwatch-based system has been used successfully in real-time to detect falls for elderly persons. We have developed and deployed a SmartFall system on a commodity-based smartwatch which has been trialled by nine elderly participants. The system, while being usable and welcomed by the participants in our trials, has two serious limitations. The first limitation is the inability to collect a large amount of personalized data for training. When the fall detection model, which is trained with insufficient data, is used in the real world, it generates a large amount of false positives. The second limitation is the model drift problem. This means an accurate model trained using data collected with a specific device performs sub-par when used in another device. Therefore, building one model for each type of device/watch is not a scalable approach for developing smartwatch-based fall detection system. To tackle those issues, we first collected three datasets including accelerometer data for fall detection problem from different devices: the Microsoft watch (MSBAND), the Huawei watch, and the Meta Sensor device. After that, transfer learning strategy was applied to first explore the use of transfer learning to overcome the small dataset training problem for fall detection. We also demonstrated the use of transfer learning to generalize the model across the heterogeneous devices. Our preliminary experiments demonstrate the effectiveness of transfer learning for improving fall detection, achieving an F1 score higher by over 10% on average, an AUC higher by over 0.15 on average, and a smaller false positive prediction rate than the non-transfer learning approach across various datasets collected using different devices with different hardware specifications.

Keywords: Fall Detection, Transfer Learning, Small Dataset

1. Introduction

Falls are one of the leading causes of death and injury among the elderly population [1]. According to the U.S. Center of Disease Control and Prevention, one in four Americans aged 65 and older falls each year [2]. A recent CDC report also stated that around 28% of people aged over 65 lived alone [3]. In addition, the Agency for Healthcare Research and Quality reports that each year, somewhere between 700,000 and 1,000,000 people in the United States fall in the hospital alone [4]. The resultant inactivity caused by a fall in older adults often leads to social isolation and increased illnesses associated with inactivity including infections and deep vein thrombosis. Consequently, a large variety of wearable devices which incorporate fall detection systems have been developed [5–8]. Wearable devices have the promise of bringing personalized health monitoring closer to the consumers. This phenomenon is evidenced in the articles entitled “Staying Connected is Crucial to Staying Healthy” (WSJ, June 25, 2015) and “Digital Cures For Senior Loneliness” (WSJ, Feb 23, 2019). The popularity of using a smartwatch, paired with a smartphone, as a viable platform for deploying

36 digital health applications is further supported by release of the Apple Series brand of smartwatches
37 [9] which has a built-in “hard fall” detection application as well as an ECG monitoring App. Apple
38 also added car crash detection in the most recently version of Apple watches. An Android-Wear based
39 commercial fall detection application called RightMinder [10] has been released on Google Play since
40 2018. One of the major sensors used in fall detection on a smartwatch is an accelerometer, which
41 measures the acceleration of an object. Acceleration is the change in velocity with respect to time and
42 velocity represents the rate at which an object changes its position. Acceleration data is commonly
43 used in fall detection because accelerometer sensors are found in most smart devices, and a distinct
44 change in acceleration happens when a fall occurs. The clustered spikes in Figure 1a show a unique
45 pattern in the acceleration data during one second when the fall occurs, which means that falls can
46 be identified in acceleration data by that pattern.

47 Previously, we have developed a watch-based SmartFall App using Long Short-Term Memory
48 neural networks (LSTM), an artificial recurrent neural network (RNN) with feedback connections,
49 to detect falls based on the above pattern, by training it on simulated fall data collected using a
50 Microsoft watch (MSBAND) [11,12]. We have deployed this SmartFall system on a commodity-based
51 smartwatch which has been trialled by nine sensor participants. Each participant was recruited under
52 IRB 7846 at Texas State University to use the SmartFall system to collect their ADLs (Activity of
53 Daily Living) data by just asking them to wear the watch for three hours per day over a seven day
54 period. The user only needs to interact with the watch and provide feedback when false positives
55 are generated by the system. Despite the system was welcomed by the participants in our trials, it
56 still have several limitations: 1) fall detection models trained on simulated falls and ADLs performed
57 by young, healthy test subjects suffer from the fact that they do not exhibit the same movement
58 characteristics as the elderly population. For example, an elderly person typically has comorbidities
59 that affect their movements including the effects of multiple medications, poor vision, stroke, arthritis,
60 sensory neuropathies and neuro-degenerative diseases such as Parkinson’s disease, all of which may
61 contribute to their risk of falling [13]; 2) a sudden hand or wrist movement from some ADLs can
62 interfere with the recognition of this pattern. For example, Figure 1b is the signal generated from a
63 person putting on a jacket and has some cluster spikes which can be mistaken for a fall; 3) there is no
64 guarantee that accelerometer data collected from different smartwatch devices is exactly of the same
65 quality for fall detection since they have different hardware characteristics and API libraries.

66 In addition, we find that a fall detection model trained with data collected using a specific
67 device usually does not generalize well to similar data collected using a different device because
68 of differences in hardware characteristics which result in the acceleration data being sensed and
69 recorded with varying G units, sampling rates, and X, Y and Z orientations of the accelerometer
70 data. For example, Huawei watch specified that data can be collected in 32 ms, but in reality, the
71 data is always collected in every 20 ms while MSBAND collects data in 32 ms as specified. To
72 tackle the aforementioned issues, we propose to use transfer learning approach to solve the small
73 dataset problem in smartwatch based fall detection system. More specifically, while collecting a large
74 amount of ADL or fall data from the elderly population is an unrealistic task (*i.e.*, the target domain),
75 collecting a small amount of everyday movement data from the elderly population is possible (*i.e.*,
76 the source domain). Therefore, the obtained model in the source domain can be utilized and retained
77 in the target domain. This will enable us to create a real-world smartwatch-based fall detection model
78 usable by older adult where we only need to collect a small amount of data to train a model tailored
79 to each of them.

80 In this paper, we first demonstrate that transfer learning is an effective strategy for overcoming
81 the small data set problem in fall detection by using data collected from the same type of device (Meta
82 Sensor) on both left and right wrists. After that, we leverage the pretrained model on one device
83 and generalize the model via transfer learning on another device. For instance, we perform a set of
84 experiments that transfer a LSTM fall detection model that we published in [11] using data collected
85 with the source MSBAND device to a target Meta Sensor device. We show that the fall detection

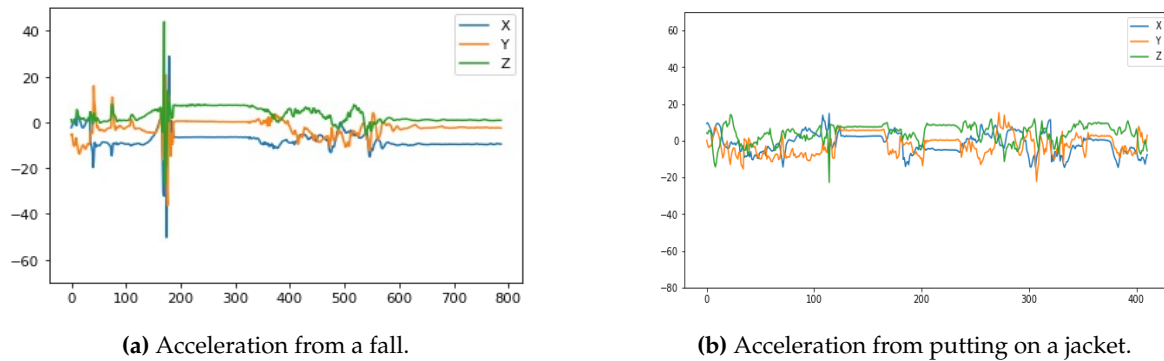


Figure 1. Comparison of smartwatch accelerometer data.

86 model created via transfer learning has a higher F1-score than the LSTM model created directly from
 87 the limited Meta Sensor data trained from scratch. We also demonstrate that another small fall data set
 88 collected using a Huawei smartwatch performed better when trained using transfer learning from a
 89 pretrained MSBAND model as well. Finally, we show that fall detection can be improved by enabling
 90 a scalable way to add new sensors to improve our fall detection system via training an ensemble of
 91 classifiers using transfer learning. For example, adding accelerometer data sensed from a cell phone
 92 might resolve the false positives generated from an ADL shown in Figure 1b. The main contributions
 93 of this paper are:

- 94 • Collecting three datasets including accelerometer data for fall detection problem from different
 95 devices: the MSBAND watch, the Huawei watch, and the Meta Sensor device.
- 96 • Conducting an in-depth study of the effectiveness of transfer learning for fall detection using a
 97 small data set by creating effective left and right wrist fall detection models.
- 98 • Exploring the practicality of applying transfer learning on heterogeneous sensing devices by
 99 transferring an existing fall detection model, trained on our MSBAND data set, to a Meta Sensor
 100 device (in one experiment), as well as a Huawei smartwatch (in another separate experiment),
 101 both using a small amount of device specific data.
- 102 • Demonstrating the improvement of fall detection using transfer learning to create an ensemble
 103 model of both left and right wrists or any additional heterogeneous sensing device.

104 The remainder of this paper is organized as follows. Section 2 describes the related work. In
 105 section 3, we discuss the architecture of the SmartFall system and the App used for running the fall
 106 detection model created by the transfer learning. In section 4, we provide the methodology used in
 107 establishing our hypothesis. This includes the detailed descriptions of how to collect three datasets
 108 from three different devices, the proposed LSTM model architecture, the tuning of hyperparameters
 109 of the LSTM model, and the transfer learning framework that was used for our experiments. In
 110 section 5, the experimental procedures and results are described and shown. Finally, section 6
 111 concludes the paper.

112 2. Related work

113 We firstly review the traditional healthcare area where transfer learning is intensively explored
 114 and then we conduct an overview of transfer learning methods with a focus on time-series data.
 115 Finally, we compare our method to the existing works which related to fall detection area, and clarify
 116 its novelties.

117 2.1. Transfer Learning for General Healthcare

118 Despite deep learning (DL) has achieved extraordinary success in a variety of tasks recently [14–
 119 16], one of the main drawbacks is DL usually relies on abundant labelled training examples. In many

120 scenarios, collecting sufficient training data is time-consuming or even impossible. Semi-supervised
121 learning method can address this problem by some extent since it only requires a limited amount
122 of labeled data [17]. However, it fails to produce a satisfactory models when unlabeled instances
123 are difficult to obtain as well. Consequently, transfer learning, which emphasizes on transferring
124 knowledge between various domains, is a promising approach to address the aforementioned
125 problem. More specifically, transfer learning aims to transfer the prior knowledge from existing
126 domains to a new domain [18]. Currently, transfer learning can be divided into two categories due
127 to the discrepancy between domains: homogeneous and heterogeneous transfer learning. In general,
128 homogeneous transfer learning approaches try to deal with the situations where the domains have
129 the same feature space. In contrast, heterogeneous transfer learning methods are proposed to handle
130 the situations where the domains have mismatched feature spaces [19].

131 Due to the fact that data collection is hard to conduct in the privacy-sensitive healthcare area,
132 extensive studies have been proposed to adopt homogeneous transfer learning to solve the data
133 scarcity issue [20–24]. For instance, Maqsood *et al.* [20] adopted and finetuned the AlexNet [25] for the
134 Alzheimer's disease detection problem. Initially, the AlexNet network is pretrained over ImageNet
135 [26] dataset (*i.e.*, the source domain) first. After that, the convolutional layers of AlexNet are fixed, and
136 the last three fully connected layers are replaced by one softmax layer, one fully connected layer, and
137 one output layer. The modified AlexNet is then finetuned on the the Alzheimer's data set [27] (*i.e.*,
138 the target domain). Results indicate that the proposed transfer learning approach retains the highest
139 accuracy for this multiclass classification problem. Similarly, Shin *et al.* [21] applied the transfer
140 learning method and finetuned the pretrained convolutional neural networks (CNN) to solve the
141 computer-aided detection problems. Moreover, Donahue *et al.* [28] proved that AlexNet [25] could
142 improve the performances of various problems, including object recognition and scene recognition.

143 In addition to the aforementioned homogeneous transfer learning methods, heterogeneous
144 transfer learning methods have been explored in healthcare area as well [29–31]. For example,
145 Palanisam *et al.* demonstrated that by applying transfer learning method, model pretrained on image
146 data, like ImageNet [26], can recognize features on non-image data like audio [29]. Specifically,
147 the audio data was converted into spectrogram images first, and the knowledge from model which
148 pretrained on ImageNet data can transfer to the spectrogram domain for audio classification problem.
149 In addition, Koike *et al.* applied transfer learning method on the heart disease prediction from heart
150 sounds [30]. They compared two transfer learning scenarios which pretrained on audio and image
151 dataset, respectively, and highlight how models pretrained on audio can outperform the one from
152 image models. In summary, it can be noted that all aforementioned works are based on the pretrained
153 models on a large-scale source domain, such as ImageNet [26] dataset.

154 2.2. Transfer Learning for Time-series Data

155 Time-series data has received huge attentions due to its robustness again various viewpoints or
156 illumination conditions [32,33]. In the healthcare domain, time-series data is also one of the most
157 common type of data. However, transfer learning techniques for time-series data have been less
158 evaluated [34–39] due to the absence of a large-scale accurately labelled dataset like ImageNet [26]
159 and the scarcity of publicly available time-series data in the healthcare domain. For instance, Li *et al.*
160 [34] developed a novel deep transfer learning technique for time-series data to use already-existing
161 datasets to overcome the target domain's data shortage problem. Initially, they have trained a deep
162 neural network (DNN) using a large number of time-series data collected from various application
163 fields so that the general properties of time-series data can be learned by this DNN model. After
164 that, they implemented the transfer learning process of this model to another DNN model which is
165 designed to solve a specific target problem. More specifically, they used a single-channel data to train
166 their single-channel DNN for sensor modality classification. After that, they built a multichannel
167 DNN [35] by fine-tuning the single-channel DNN for each channel on the target domain and thus
168 the final multichannel DNN can recognize the outputs from all channels on the target domain. They

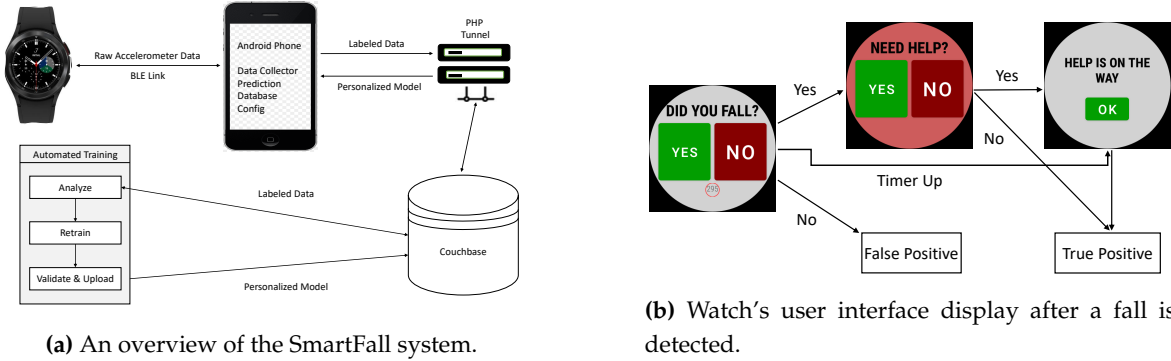


Figure 2. Architecture of SmartFall system.

evaluated their approach for human activity recognition (HAR) and emotion recognition (ER), and results confirmed that transfer learning strategy performs better than the baseline for both HAR and ER problem. Similarly, Gikunda *et al.* [36] adopted transfer learning as well as active learning to address this same problem of insufficiency of labelled time-series data. Results indicated that using only 20% of the training data, they achieved higher accuracy with hybrid transfer active learning than with existing techniques. More recently, Zhou *et al.* [38] proposed a novel dynamic transfer learning-based time-series prediction to address the issue of small datasets in industrial production. The proposed dynamic transfer learning framework was created using two features: feature mapping, and network structure. Results showed that when compared to the approach without transfer learning, the application of source domain knowledge can greatly improve target domain prediction performance in this dynamic transfer learning method. There are very few works that have explored transfer learning in a domain like a fall detection [39]. For example, Villar *et al.* [39] proposed a supervised fall detection model using online learning and transfer learning. They found that designing the fall detection specifically for each user rather than acquiring generalized models can lead to higher performance.

In summary, one of the common challenges that all of these previous works have faced is the scarcity of time series data and most of them implemented transfer learning to overcome this issue. However, none of them demonstrated the feasibility of transfer learning for overcoming the small data set problem in a real-world fall detection App. In addition, our study also explore the practicality of applying transfer learning on heterogeneous sensing devices using the same type of data collected from three different devices. This paths the way to overcome high false rates by placing more than other accelerometer sensors in different location of the human body.

3. SmartFall System Architecture

We implemented a three-layered architecture which has the smartwatch on the edge, the smartphone in the middle layer, and the cloud server in the inner most layer. This is one of the most flexible architectures for IoT applications as discussed in [40] and is a practical choice for our prototype. Microservice is a particular implementation of the service-oriented architecture (SOA) that enables an independent, flexible, and distributed ways of deployment of services on the internet. Applications designed with microservices contain small, modular, and independent services which communicate via well-defined APIs. As compared to the 3-layer architecture of our SmartFall, microservices are more agile, flexible, and resilient. However, each microservice must be hosted in a container and connected to a cloud framework. Moreover, the portability of an edge container is not proven yet. Currently, there are no Docker-compatible containers that can run on an edge device like an Android phone. We have explored a microservice-based architecture called Accessor-based Cordova host for edge devices in [41].

204 Figure 2a gives an overview of the SmartFall fall detection system. The major software
205 components developed on a smartphone are (a) the *Config* module which manages the parameters,
206 version of the deep learning model used by a particular user, the chosen personalization training
207 strategy, and the chosen cloud server for data storage and re-training; (b) the *Database* module which
208 manages all the data sensed, the uploading of the collected data to the cloud, and the downloading
209 of the best re-trained model for a user; (c) the *Data Collector* module which manages the transfer of
210 sensed data on the smartwatch to the smartphone using different communication protocols. Our
211 smartwatch and smartphone currently communicate using BLE. The smartwatch and the server
212 communicate using HTTP. Our system is designed to leverage multiple communication protocols;
213 and (d) the *Prediction* module, which manages different machine learning models used for fall
214 detection. For example, the system can be configured to run an ensemble recurrent neural network
215 (RNN) or a single RNN model. On the cloud, additional software components for analysis, re-training
216 and validation of the re-trained models are implemented. Our system is designed to be flexible for
217 using different personalization strategies as and when they become available.

218 The smartwatch's UI is designed to start with just the "YES" and "NO" buttons so as to overcome
219 the constraint of small screen space (see Figure 2b). If the user answers "NO" to the question "DID
220 YOU FALL?", the data is labelled as a false positive and stored as "FP" in the Couchbase database in
221 the cloud. If the user answers "YES", the subsequent screen will prompt "NEED HELP?". If the user
222 presses "YES" again, it implies that a true fall is detected and that the user needs help. The collected
223 data will be labeled and stored as "TP" and "HELP IS ON THE WAY" screen will be displayed. If the
224 user presses "NO", it suggests that no help is needed and the collected data is still labelled as "TP".
225 If the user did not press either "YES" or "NO" after a specified period of time following the question
226 "DID YOU FALL?", an alert message will be sent out automatically to the designated caregiver.

227 Our system is structured such that all user-identifying data is only stored locally on the phone to
228 preserve privacy. Real-time fall prediction is performed on the phone to reduce the latency of having
229 to send data to the cloud for prediction. The training/re-training of the prediction model is done
230 offline in the cloud server. The UI interface is designed such that there is no need to interact with the
231 App unless the system detects that a fall has occurred, in that case, the watch will vibrate to alert the
232 user that a prediction has occurred and the UI in Figure 2b will appear. The ability to interact with
233 the system when a false prediction is generated allows the system to collect real-world ADL data and
234 fine tune the fall detection model.

235 The ultimate goal is for the system to detect falls accurately, i.e. not missing any falls and not
236 generating too many false positive prompts. Collecting data and training a new model from scratch
237 is labour intensive, hence, we aim to have one model that can generalize well across different smart
238 devices. When a new device is added, by using a small amount of feedback data collected by the user
239 wearing the device for a short period of time, a new model can be trained with a transfer learning
240 strategy and uploaded to the device to use in real-time. The following sections describe the transfer
241 learning experiments we conducted to support our vision in this SmartFall system.

242 4. Methodology

243 4.1. Dataset Collection

244 We first collected three datasets which can be used in the transfer learning experiments. Those
245 datasets are comprised of accelerometer data collected from the Microsoft watch (MSBAND) watch,
246 the Huawei watch, and the Meta Sensor device. MSBAND and Huawei data were collected in units
247 of 1G on the left wrist only, while Meta Sensor data was collected in units of 2G on both the left and
248 right wrists. The sampling rate is 32 Hz for MSBAND and Huawei watches while Meta Sensor data
249 is collected with the sampling rate of 50 Hz. Figure 3 shows the three different devices we used for
250 the data collection process.

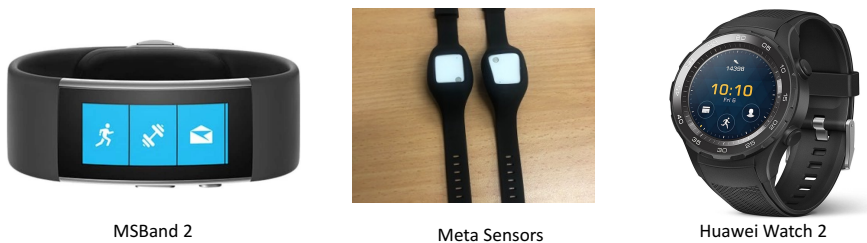


Figure 3. The three different hardware used for data collection.

251 The MSBAND dataset was collected from 14 volunteers each wearing a MSBAND watch. These
 252 14 subjects were all of good health and were recruited to perform a mix of simulated falls and ADLs
 253 (Activity of Daily Living). Their ages ranged from 21-55, height ranged from 5 ft to 6.5 ft. and weight
 254 from 100 lbs to 230 lbs. Each subject was told to wear the smartwatch on his/her left wrist and
 255 perform a predetermined set of ADLs consisting of: walking, sitting down, picking up an object,
 256 and waving their hands. This initial set of ADLs were chosen based on the fact there were common
 257 activities that involved movement of the wrists. Those data were all labelled as "NotFall". We then
 258 asked the same subjects to perform four types of falls onto a 12-inch-high mattress on the floor;
 259 front, back, left, and right falls. Each subject repeated each type of fall 10 times. We implemented
 260 a data collection service on an Android phone (Nexus 5X, 1.8 GHz, Hexa-core processors with 2G of
 261 RAM) that paired with the MSBAND smartwatch to have a button that, when pressed, labels data
 262 as "Fall" and otherwise "NotFall". Data was thus labelled in real-time as it was collected by the
 263 researcher holding the smartphone. This means when the user was walking towards the mattress
 264 before falling down or getting up from each fall, those duration of data will be labelled as 'NotFall'.
 265 However, the pressing of the button can introduce errors such as the button is being pressed too
 266 late, too early, or too long for a fall activity. To mitigate these errors, we post-processed the collected
 267 data to ensure that data points related to the critical phase of a fall were labeled as "Fall". This
 268 is done by implementing an R script that will automatically check that for each fall data file, the
 269 highest peak of acceleration, and data points before and after that point, were always labeled as
 270 "Fall". After this post-processing of the collected data, we have a total of 528 falls and 6573 ADLs.
 271 The MSBAND watch was decommissioned by the vendor in May 2019. This dataset is available
 272 <http://www.cs.txstate.edu/~hn12/data/SmartFallDataSet.zip>.

273 Huawei watch is compatible with Android WearOS and we designed and implemented an
 274 Activity Labelling App on both the watch and the Android phone for data collection. This activity
 275 labeler consists of two components: one on the phone and one on the watch. The watch paired with
 276 the phone using Bluetooth and collects, labels, and sends accelerometer data to the phone in real time.
 277 The phone is considered as a gateway device where labeled data can be stored temporary and then
 278 uploaded to a remote cloud server periodically. The App records accelerometer data sensed from
 279 the Huawei watch with a start and stop button, and a user can enter what kind of activity is being
 280 recorded before pressing the start button so that the data comes out labeled with a specific activity
 281 name rather just "NotFall" as compared with the MSBAND dataset. Twelve students including 7
 282 males and 5 females were asked to perform a prescribed list of ADL activities in triplicate and each
 283 type of fall five times. Their ages range from 21 to 35 and their weight average from 100 to 150 lbs.
 284 Each participant performed five different type falls on an air mattress - front, back, right, left and
 285 rotate fall. They were also asked to perform 6 different types of ADL tasks - walking, waving hand,
 286 drinking water, wearing a jacket, sitting down and picking stuff from floor. Collected data were
 287 preprocessed to trim the initial and ending data segment to account for the human errors in pressing
 288 or releasing the buttons and to segment the activities and falls into individual trial for training (since
 289 each activity is performed 3 times and each type of fall is performed 5 times). The fall data is further
 290 processed into equal sequence of 100 data points for each fall data sample and multiple of 100 data
 291 points for each ADL data sample. Not all data collected were usable due to missing data points in

292 some falls and ADLs. The final dataset after preprocessing has 144 falls and 271 ADL samples, and is
293 available at http://www.cs.txstate.edu/~hn12/data/Huawei_7030.zip.

294 Meta Sensor was developed by MBIENTLAB in San Francisco(mbientlab.com). It is a wearable
295 device that offers continuous sensing of motion and environment data. It can sense gyroscope,
296 accelerometer and magnetometer, and it provides easy-to-use open source APIs for fast data
297 acquisition. Data can be stored locally on the phone or in a cloud server provided by MBIENTLAB. The
298 Meta Sensor we used is the MetaMotionRL. The sensor has a weight of 0.2 oz and can be recharged
299 via USB port. By embedding the meta sensor in an appropriate wrist band, it can serve as a wrist
300 watch for easy collection of ADLs and simulated fall data. The collected data can be exported into
301 multiple file formats. We recruited 8 participants (3 male and 5 female) with ages from 22 to 62 for
302 data collection. Each participant is asked to perform four types of fall (front, back, left and right), five
303 time each on an air mattress, and a prescribed list of ADLs as in the Huawei watch data collection
304 session. These are walking, waving hand, drinking water, wearing a jacket, sitting down and picking
305 stuff from the floor.

306 The Meta Sensor fall data was first programmatically labeled by a Python script that identifies a
307 set amount of peak magnitudes based on the amount of trials per file and a uniform width of 35 data
308 points (1.12 seconds) per fall. Plotting programmatically labelled Meta Sensor data in Microsoft Excel
309 showed that labels were often placed around peaks caused by noise rather than actual falls and did
310 not capture the distinct pre-fall, fall, and post-fall activity that accompanied an actual fall. To ensure
311 that we have a set of accurately labelled Meta Sensor data to experiment with, we decided to manually
312 relabel all Meta Sensor data using Excel plots as a basis for fall window placement. We choose fall
313 windows with a width of 100 data points in attempt to capture both pre-fall and post-fall activities. To
314 minimize noise, we trimmed non-fall data in between each fall. Since an ADL activity could last much
315 longer than a fall, we label the non-fall data in ADL files to the smallest multiple of 100 data points
316 per trial that could capture the entire activity being performed. The collected Meta Sensor data has
317 202 falls and 492 ADL samples, and is available at http://www.cs.txstate.edu/~hn12/data/Meta_sensor_7030.zip.

319 4.2. Experimental Settings

320 Transfer learning is a research subject in machine learning that is concerned with the transfer
321 of knowledge obtained while training a model for a specific task, and applying that knowledge as
322 a base model to a different but related task [18]. For ease of understanding, we select one of our
323 experiments to explain how the transfer learning strategy works in this study. Initially, we use the
324 MSBAND dataset, which we call the **source dataset**, to train a model from scratch, in turn giving us
325 our preliminary knowledge in the shape of a model that is fully trained to solve the fall detection
326 problem on data sensed by the MSBAND. After that, we use that model as a base model for the Meta
327 Sensor dataset, which we call the **target dataset**, by freezing all of its precursory layers, effectively
328 keeping the weights that resulted from the MSBAND dataset training process as is, and re-training
329 only the dense layers of the model on the Meta Sensor dataset. The intuition behind it comes from
330 the small size of the retraining dataset, as the base model resulted from training on a bigger, more
331 complete dataset, making it more desirable in its complex, initial layers, while at the same time
332 transferring over the knowledge needed to normalize the data in the dense layers with respect to
333 the differences between the two datasets. The full transfer learning process is described in algorithm
334 1. In the algorithm, we have the source and target datasets as the input. We start off by organizing
335 the data into windows (data windows are explained in section 4.3) and initializing two models, one
336 suffixed with TFS (Training From Scratch), and the other is suffixed with TL (Transfer Learning). We
337 train the TL model on the full source dataset and freeze its precursory layers, and then evaluate the TL
338 and TFS models on the target dataset by conducting experiments described in section 5, and compare
339 the performance of the two models in those experiments. All our experiments are conducted on a
340 Dell Precision 7820 Tower, 256 GB RAM and one GeForce GTX 1080 GPU using TensorFlow.

Algorithm 1 Our Transfer Learning Structure

Input: Source Domain Data *Source_Data*, Target Domain Data *Target_Data*

Organize *Source_Data* And *Target_Data* Into Data Windows

Initialize Models *NN_TL* And *NN_TFS*

Train *NN_TL* On *Source_Data* Data Windows

Freeze *NN_TL*'s Precursory Layers

Evaluate *NN_TL* And *NN_TFS* On *Target_Data* Data Windows

Compare The Evaluation Results Of *NN_TL* And *NN_TFS* On *Target_Data*

341 4.3. *Model Training and Parameters Tuning*

342 As mentioned before, we used a simple LSTM neural network structure for our model, as not
343 only does that fit the time-series task well, but it is also a viable option for real-time classification that
344 operates on the edge device without having the need to communicate to the cloud. Our classifier
345 had many different hyperparameters, as well as different options for layer structuring, all of which
346 needed extensive tuning in order to find which permutation of these hyperparameters and structures
347 gives the best result. The main hyperparameters for our classifier are:

- 348** • **Window_Size:** The number of consecutive data entries that will be fed to the LSTM classifier
349 at once. For example, if the window size is 35 (meaning the length of a single input block is 35
350 time-consecutive data entries), then the classifier will be fed a tensor of the shape 35x3 (since
351 we have 3 coordinates for acceleration for each entry) to give a single classification for. This
352 snapshot of a particular window size represents one sample of time series data as shown in
353 Figure 1a.
- 354** • **Step_Size:** The difference between two consecutive data **blocks** (each block comprised of
355 **Window_Size** data entries). For example, say we have 37 data entries, with a **Window_Size**
356 of 35 and a **Step_Size** of 1, then, we would have 3 different data blocks, them being [1, 35],
357 [2, 36] and [3, 37], which means we have an overlap of 34 entries between each 2 consecutive
358 data entries. If **Step_Size** was 2, then we would have 2 different data blocks, them being [1,
359 35] and [3, 37] (the middle block would be skipped since our step is 2), with an overlap of 33
360 entries between each 2 consecutive entries (**Window_Size - Step_Size** is the general number of
361 overlapping entries).
- 362** • **Smooth_Window:** The way we have our model make a final prediction is by predicting over
363 the last **Smooth_Window**: data blocks, and then average (take the median of) the predictions
364 and use that average as the final fall probability. The motivation behind the smooth window
365 is to take into account a wider scope of predictions, better covering pre-fall and post-fall data
366 points. This will also ensure that we do not miss any clustered spikes related to fall and we do
367 not just take a single spike as a fall prediction.
- 368** • **Fall Threshold:** After having the averaged fall probability from the most recent smooth
369 window, if its value is greater than **Fall Threshold**, then we classify the window as a fall,
370 otherwise we classify it as a non-fall.

371 As mentioned above, the hyperparameter tuning process needed an extensive amount of
372 experimentation, and for each hyperparameter we tried a multitude of different numbers from lower
373 to higher values. In this part of the sub-section, we will be describing the experimentation process
374 for each hyperparameter and mentioning what the optimal value is with the reasoning behind it. The
375 hyperparameter tuning process was validated on the MSBAND and Meta Sensor datasets, for each
376 dataset separately, by splitting that dataset into a training set, which consisted of 70% of the data, and
377 a test/validation set, which consisted of 30% of the data. For each choice of hyperparameters, we
378 would train our classifier on the training set, and then calculate the **F1 score** of the trained model on
379 the test set. In the results tables, we show the scores of 5 different values as the other values' results
380 were similar to the value closest to them in the table.

381 • **Window_Size:** We tried a multitude of different values, and found that the optimal value is the
 382 same as the number of data entries sensed within 1 second (the duration of a fall), meaning that
 383 the optimal value for the MSBAND model was **32**, as the MSBand is at 32 Hz, and the optimal
 384 value for the Meta Sensor model was **50**, as the Meta Sensor is at 50 Hz. This seemed to be the
 385 sweet-spot that captures enough data for an accurate classification, any value below that gave
 386 a worse classification accuracy, and any value beyond that did not increase the classification
 387 accuracy by a noticeable amount.

Table 1. Window_Size tuning for MSBAND and Meta Sensor datasets respectively

Value	15	20	32	40	50
F1-Score	0.8	0.85	0.93	0.91	0.92

Value	30	40	50	60	70
F1-Score	0.75	0.76	0.81	0.81	0.8

388 • **Step_Size:** Out of all the values, a step of 1 seemed to perform the best, which indicates that
 389 high overlap and small increments between the consecutive data blocks is important for a good
 390 performance, as all the higher values gave worse results.

Table 2. Step_Size tuning for MSBAND and Meta Sensor datasets respectively

Value	1	3	5	7	9
F1-Score	0.93	0.9	0.87	0.88	0.86

Value	1	3	5	7	9
F1-Score	0.81	0.77	0.79	0.75	0.73

391 • **Smooth_Window:** As explained before, we want to capture the notion of both pre-fall and
 392 post-fall occurrence in order to help us better classify falls and have less false positives, and
 393 exactly matching that intuition, a broader smooth window of about 2 seconds of sensed data
 394 entries (64 for MSBand and 100 for Meta Sensor) out-performed both shorter and longer smooth
 395 windows.

Table 3. Smooth_Window tuning for MSBAND and Meta Sensor datasets respectively

Value	20	40	64	80	100
F1-Score	0.83	0.89	0.93	0.86	0.87

Value	20	60	100	130	160
F1-Score	0.69	0.75	0.81	0.75	0.78

396 • **Fall_Threshold:** Different values in increments of 10% were tried, starting from 10% and ending
 397 at 90%, and the fall threshold of 40% performed the best as it had the best balance of accurate
 398 true-positive classification while avoiding as many false-positives as possible. This value wasn't
 399 picked solely through experimentation, but also by looking at the prediction probability of the
 400 classifier over the test set, we can see that for the fall data, the classifier predicts values above
 401 40%, and for non-fall data, it predicts values below 40%.

Table 4. Fall_Threshold tuning for MSBAND and Meta Sensor datasets respectively

Value	0.1	0.3	0.4	0.7	0.9
F1-Score	0.68	0.85	0.93	0.81	0.67

Value	0.1	0.3	0.4	0.7	0.9
F1-Score	0.6	0.76	0.81	0.73	0.65

402 As we have mentioned, not only did we tune the hyperparameters of the network, we also tried
 403 several structures for the network itself, mainly following the LSTM layer, as a part of our model
 404 tuning. Previous work's benchmark model is illustrated in Figure 4a.

405 As we can see, the model consisted of an LSTM layer, followed by a dense layer, batch
 406 normalization and ended off with another dense layer. It worked well as is, however, through

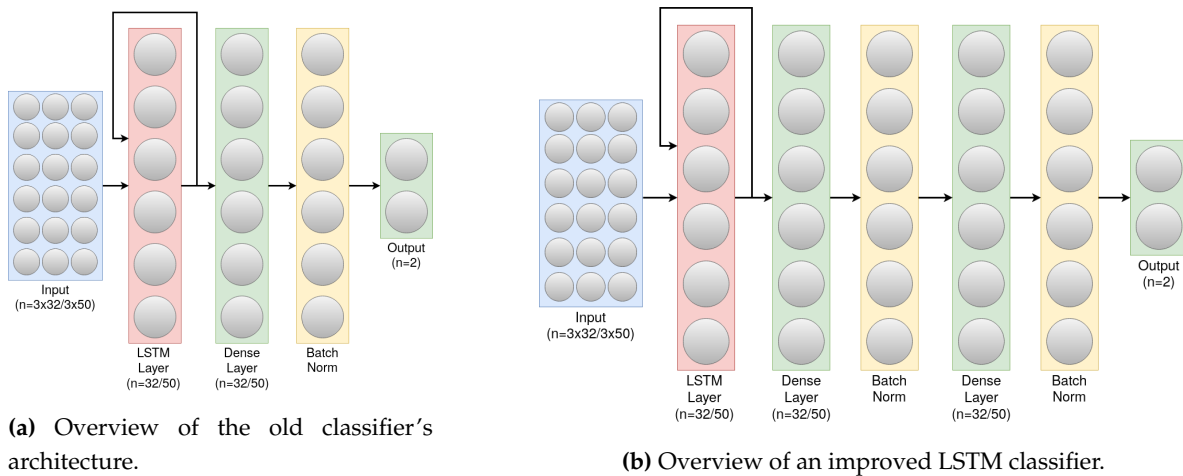


Figure 4. Comparison of classifier architectures.

407 examining the training accuracy during the training process, the accuracy value seemed to plateau
 408 earlier than desired, which is what led to experimenting with the network structure by adding more,
 409 but not too many, additional dense layers, up to a point where it wouldn't impact the classification
 410 time, and enough to be able to overcome the training accuracy plateau as well as achieve better test
 411 accuracy. And indeed, after thorough experimentation, a more optimal structure was achieved, one
 412 that had more parameters (from 13,601 to 16,351 parameters), hence more potential for knowledge
 413 gain, while maintaining relatively quick classification speed. The new structure simply had 2
 414 additional layers, a batch normalization layer followed by a dense layer. The structure of the new
 415 model can be seen in Figure 4b. It is worth noting a few things that are consistent between our model
 416 and the previous work's model:

- 417 • All layers are fully connected, using drop-out/convolution layers made the performance of the
 418 model slightly worse, hence why we do not use any of those layers.
- 419 • The activation function of the dense layers is Relu, and the last layer uses Sigmoid which is
 420 commonly used for binary classification.
- 421 • The default Keras Library's Binary Cross-Entropy loss function as well as the default Adam
 422 optimizer were used as the loss function and optimizer of the network, as those two worked
 423 well in our older version of classifier.
- 424 • The number of neurons in the LSTM layer, as well as the output dimensions of the Dense layers
 425 were always set to the number of data entries sensed in one second, similarly to **Window_Size**,
 426 as that generally gave the best result.

427 5. Experiments and Results

428 In this section, we present our experimental results on transfer learning between the several
 429 datasets we described above, being the MSBAND dataset, the Meta Sensor dataset, and the Huawei
 430 dataset. We conduct two main experiments across each pair of datasets. In one of the experiments,
 431 we have a **source** dataset and a **target** dataset. We start off by building a model from scratch on the
 432 **target's** training dataset, and then testing out that model's performance on the **target's** test dataset.
 433 We then build a model using the **source's** complete dataset, and then use that model as a base model
 434 for the **target's** training dataset, test it out on the **target's** test dataset, and compare the performance
 435 of the two results. In the second experiment, we split the **target** dataset such that each person's data
 436 is in one data fold, meaning that if we have **n** different people who volunteered to collect data for a
 437 specific dataset, we would split that dataset into **n** different folds, and conduct a cross validation on
 438 those folds, the first cross validation being from scratch, and the second cross validation having the
 439 **source's** model as a base model for each iteration. This form of leave one out cross validation is more

440 rigorous when the dataset is small. The models' structures throughout our experiments will all be the
441 exact optimal structure described in the previous section in Figure 4b, as that structure, as explained,
442 performed the best across all three different datasets, while each dataset's hyperparameters will be
443 specific to that dataset's smart watch's hardware specifications, as detailed in section 4.3.

444 *5.1. Left Wrist to Right Wrist Transfer Learning with Meta Sensor*

445 Our first set of experiments involved purely the Meta Sensor dataset, as we wanted to test out
446 the effect of transfer learning when the sensing models share identical hardware specifications, but
447 are however applied to different wrists. We started off by building a left wrist fall detection model,
448 training it from scratch using the left wrist Meta Sensor dataset, using the optimal network structure
449 and hyperparameters choice, which resulted in a fall detection model tailored specifically for the left
450 wrist. Then, using that model, we conducted two different experiments in order to evaluate the effect
451 of transfer learning in the manner described in the beginning of section 5, which we detail more
452 thoroughly below.

453 1. **Meta Sensor Experiment I:** In the first of the two experiments, we split the right wrist's dataset
454 into two sets, one of them being a training dataset comprised of 70% of all the data, and the
455 remaining 30% are the test dataset. The content of the two datasets was such that for each
456 of the 8 people in the full dataset, 70% of that person's data was in the training set, and the
457 remaining 30% was in the test set, which means that this experiment's main goal is to try and
458 evaluate how well does the model personalize to these specific 8 people after seeing a portion
459 of their data during the training process. After splitting the data in the described manner, we
460 built two different classifiers using the right wrist training data, the first of which was built
461 from scratch using the right wrist training dataset only. The second classifier was built using
462 transfer learning by having the left wrist classifier as a base model, and then training that base
463 model on the right wrist training dataset. Results are presented in Figure 5. We can clearly
464 see the effectiveness of transfer learning over building a model from scratch throughout all 3
465 presented metrics. If we look at the PR curve, we can see that the transfer learning model's PR
466 curve is more complete and covers more area resulting in a higher AUC. We then evaluated
467 both classifiers' performance on the right wrist test dataset.

468
469 If we look at the prediction probabilities plot, we can see similar true positive classifications
470 between the two models (keep in mind that the prediction threshold for a fall is 0.4), however,
471 we can also see that the transfer learning model has fewer false positive classification instances,
472 for example, if we look at the entries from 12k to 15k in the x axis, we can see that the non
473 transfer learning model predicted them falsely as falls (the real label is in **blue**, the predicted
474 value is in **red**, a red value higher than 0.4 means a fall prediction), while the transfer learning
475 model predicted them correctly as non-falls. Finally, If we look at the F1 scores, we can see
476 that the transfer learning model achieved an F1 score that is higher by 8% than the non transfer
477 learning model as shown in Table 5.

478 2. **Meta Sensor Experiment II:** In this experiment, we conducted what we call a
479 leave-one-person-out cross validation, which, as its name suggests, is a cross validation method
480 in which, for each person involved in the Meta Sensor dataset, we train the model either from
481 scratch, or using the transfer learning methodology, on a dataset that is comprised of all the
482 people but the one specific person, and then test the resulting model on the remaining person's
483 data. As mentioned, we do this process for each of the 8 people involved in the full Meta Sensor
484 dataset. As opposed to the first experiment, when testing a model in this experiment, the model
485 would have not trained on any data of the person it is being tested on.

486 The result of training and testing using leave-one-out strategy is shown in Figure 6. The
487 PR Curve and Prediction plots are taken from a random iteration of the cross validation

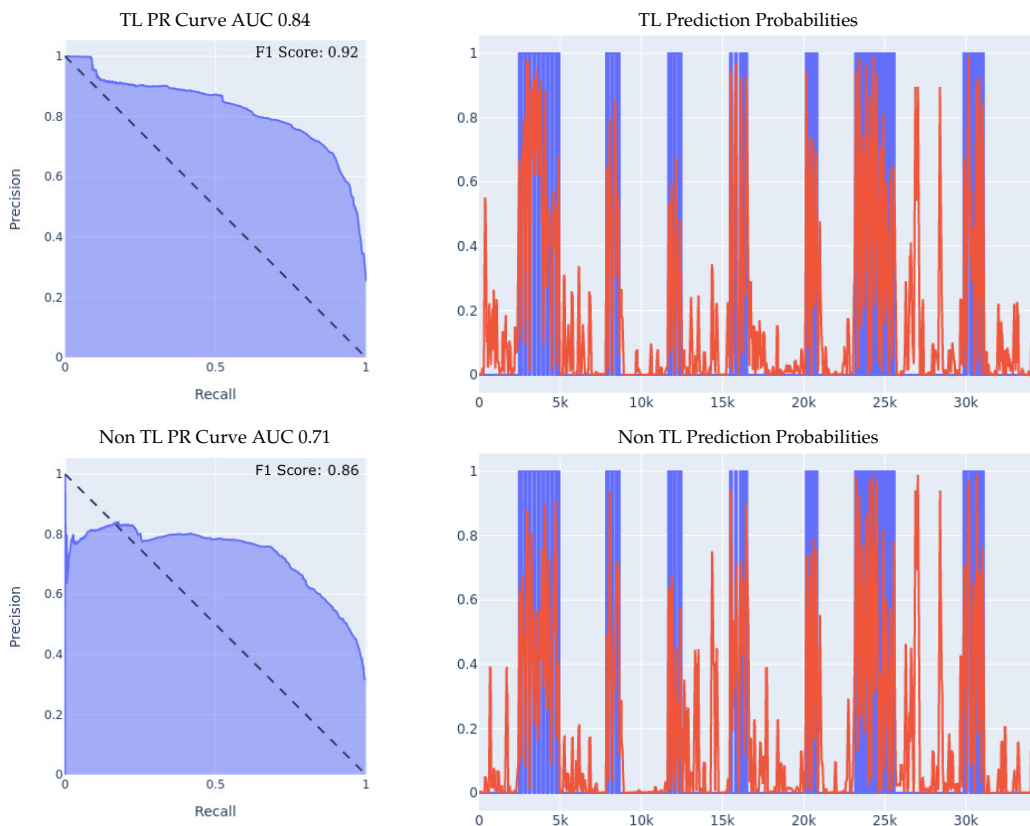


Figure 5. 70/30 Train/Test Data Split Experiment for Meta Sensor. Note that, **TL** stands for Transfer Learning, for prediction probabilities, x axis is the time, y axis is the prediction threshold, blue data is the real labels, red data is the prediction probabilities.

process, and are representative of the average iteration. The evaluation results of a single iteration are based on a dataset of one person only, hence the number of data entries in the leave-one-person-out cross evaluation results are always significantly less than the prior 70/30 Train/Test experiment, as the evaluation results in that experiment are on 30% of the entire dataset. Again, we can clearly see the effectiveness of transfer learning over building a model from scratch throughout all 3 presented metrics. If we look at the PR curve, we can see that the transfer learning model's PR curve is more complete and covers more area resulting in a higher AUC, even though both models do not achieve the best result, however, the improvement from using transfer learning is substantial, as it made the PR curve over half of the area, while in the non transfer learning case, it covered less. If we look at the prediction probabilities plot, we can see similar true positive classifications between the two models with the transfer learning model being slightly better, and we can see that the non transfer learning model has many more prediction peaks and much sharper spikes in the non-fall area, resulting in more false positive predictions. Finally, If we look at the F1 Scores, we can see that the transfer learning model achieved an averaged F1 score that is higher by almost 10% than the non transfer learning model as shown in Table 5.

5.2. MSBAND to Meta Sensor/Huawei Transfer Learning

Our second set of experiments involved two different inter-device transfer learning experiments. As the main thing we want to test out in our experiments is the effect of transfer learning on small dataset problems, the source of the transfer learning process, aka the base model, is built from training on the Microsoft band dataset, as the MSBAND dataset is the biggest and most complete dataset out

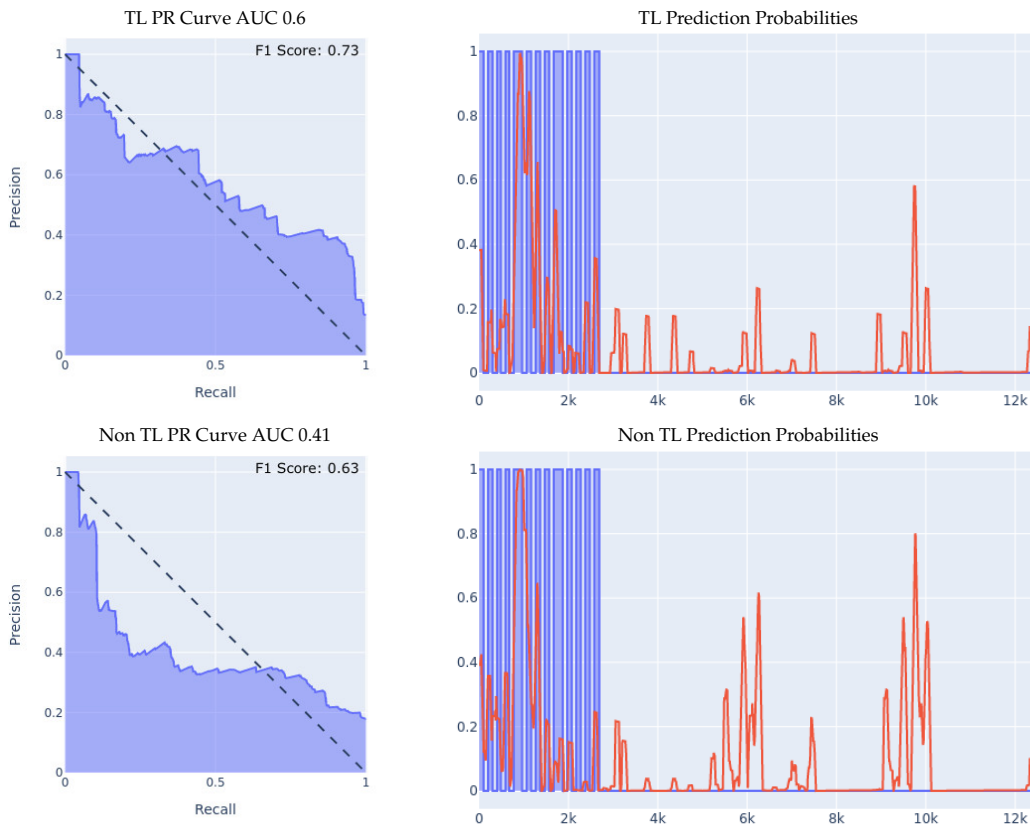


Figure 6. Leave-One-Person-Out Data Split Experiment for Meta Sensor. For prediction probabilities, x axis is the time, y axis is the prediction threshold, blue data is the real labels, red data is the prediction probabilities. For the F1 Scores, the averaged F1 score of all the 8 iterations of the cross validation is shown in the top right corner of the PR curve

509 of the three, while the Meta Sensor dataset as well as the Huawei dataset are both smaller in size and
 510 in fall samples.

511 5.2.1. MSBAND to Meta Sensor

512 As described above, we started off by training a fall detection model from scratch, using the
 513 optimal network structure and hyperparameters choice, on the MSBAND dataset, which resulted in
 514 a fall detection model tailored specifically for the MSBAND device, and then, using that model, we
 515 conducted two different experiments on the **left** wrist Meta Sensor dataset similarly to what we did
 516 in section 5.1.

517 1. **MSBAND to Meta Sensor Experiment I:** In this experiment, we conduct the exact same 70/30
 518 Train/Test split experiment as we did in the first experiment of section 5.1. The classifiers'
 519 performance on the left wrist dataset is shown in Figure 7.

520 We can see the effectiveness of transfer learning over building a model from scratch throughout
 521 all 3 presented metrics. If we look at the PR curve, we can see that the transfer learning model's
 522 PR curve is slightly more complete and covers more area resulting in a higher AUC. If we look
 523 at the prediction probabilities plot, we can see that the transfer learning model has fewer false
 524 positive classification instances, for example, if we look at the entries from 13k all the way
 525 up to 23k in the x axis, we can see that the non transfer learning model predicted a lot of the
 526 non-fall entries as falls, while the transfer learning model predicted them correctly as non-fall,
 527 resulting in a much lower false positive rate. Finally, If we look at the F1 Scores, we can see that
 528 the transfer learning model achieved an F1 score that is higher by 12% than the non transfer
 529 learning model, breaking into the 90% range as shown in Table 5.

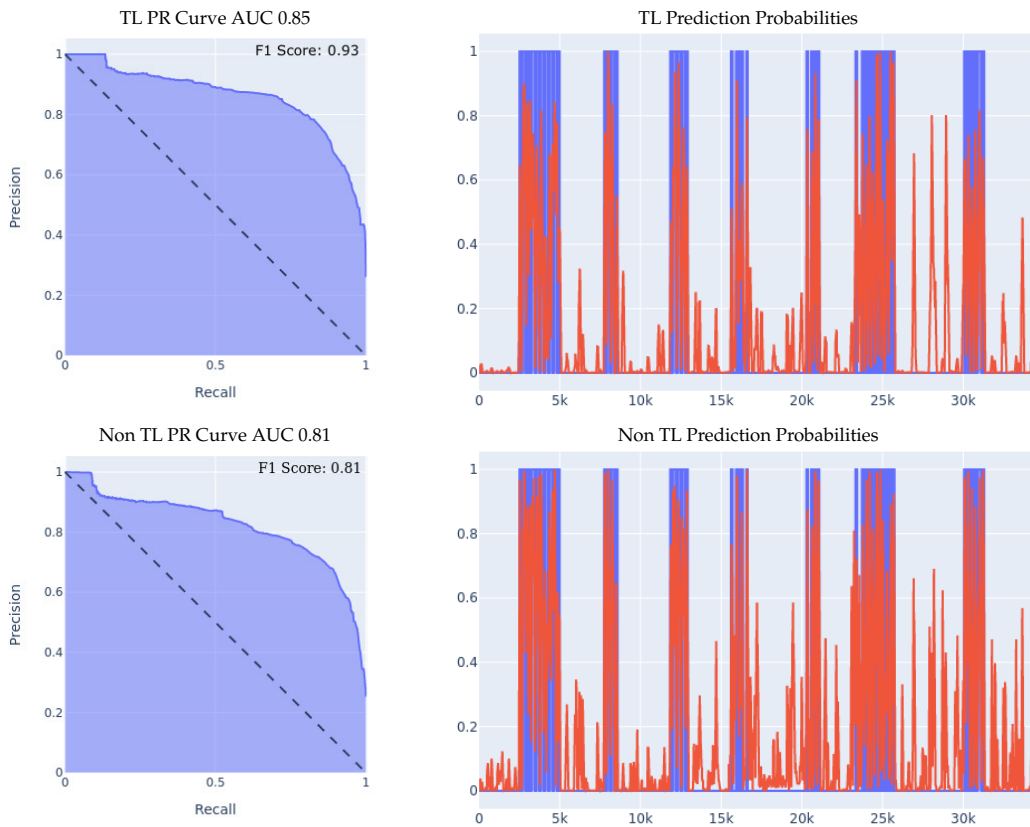


Figure 7. 70/30 Train/Test Data Split Experiment for MSBAND to Meta Sensor. For prediction probabilities, x axis is the time, y axis is the prediction threshold, blue data is the real labels, red data is the prediction probabilities

530 2. **MSBAND to Meta Sensor Experiment II:** We conduct the exact same leave-one-person-out
 531 cross validation experiment as we did in the second experiment of section 5.1 with the MSBAND
 532 and left Meta Sensor datasets.

533 We compare the results of the two models as shown in Figure 8. The results we obtained show
 534 an even higher gap between the transfer learning model and the non transfer learning model
 535 than the experiment we reported in section 5.1. Again, we can clearly see the effectiveness of
 536 transfer learning over building a model from scratch throughout all 3 presented metrics. If
 537 we look at the prediction probabilities plot, we can see that the non transfer learning model
 538 has many more prediction peaks and much sharper spikes in the non-fall area, resulting in
 539 more false positive predictions in the non transfer learning case. The F1 Scores with the transfer
 540 learning is higher by over 14% than the non transfer learning model in this experiment as shown
 541 in Table 5.

542 5.2.2. MSBAND to Huawei

543 We conducted three experiments on the Huawei dataset, the first two experiments being the
 544 70/30 Train/Test split and the leave-one-person-out experiments described in section 5.1, and the
 545 third experiment is a real-time test of the transfer-learning model by one lab volunteer. The real-time
 546 test involves wearing the Huawei watch running the SmartFall App described in section 3 using a
 547 model trained with and without transfer learning.

548 1. **MSBAND to Huawei Experiment I:** the results of the 70/30 Train/Test experiment are
 549 presented in Figure 9. We can see the effectiveness of transfer learning over building a model
 550 from scratch throughout all 3 presented metrics.

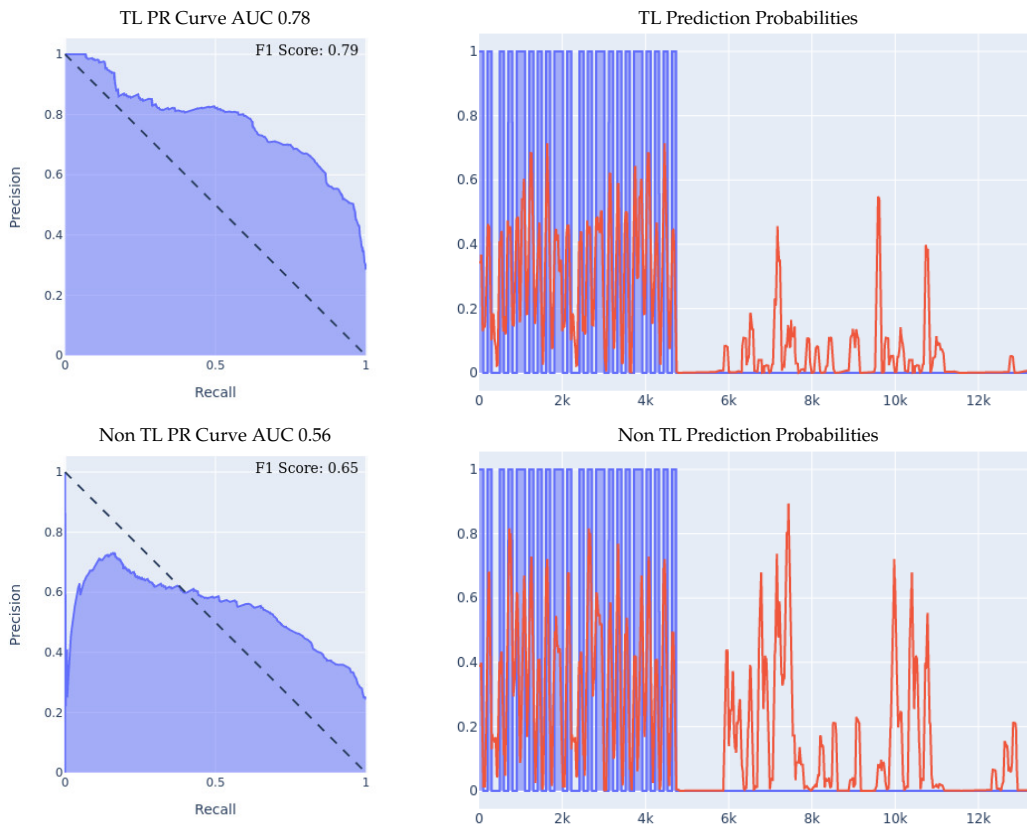


Figure 8. Leave-One-Person-Out Data Split Experiment for MSBAND to Meta Sensor. For prediction probabilities, x axis is the time, y axis is the prediction threshold, blue data is the real labels, red data is the prediction probabilities. For the F1 Scores, the averaged F1 score of all the 8 iterations of the cross validation is shown in the top right corner of the PR curve

552 If we look at the prediction probabilities plot, we can see that the transfer learning model has
 553 fewer false positive classification instances, for example, if we look at the entries from 12k to
 554 15k on the x axis, we can see that the transfer learning model has much less false positive
 555 predictions. The transfer learning model achieved an F1 score that is higher by 14% than the
 556 non transfer learning model as shown in Table 5. Note that in the transfer learning case, the F1
 557 score isn't as high as the AUC might imply, and that is because the F1 score is a metric that is
 558 focused on the false positive rate and not on the general accuracy, which is an important metric
 559 for our evaluation, since false positives are a big limitation for our problem.

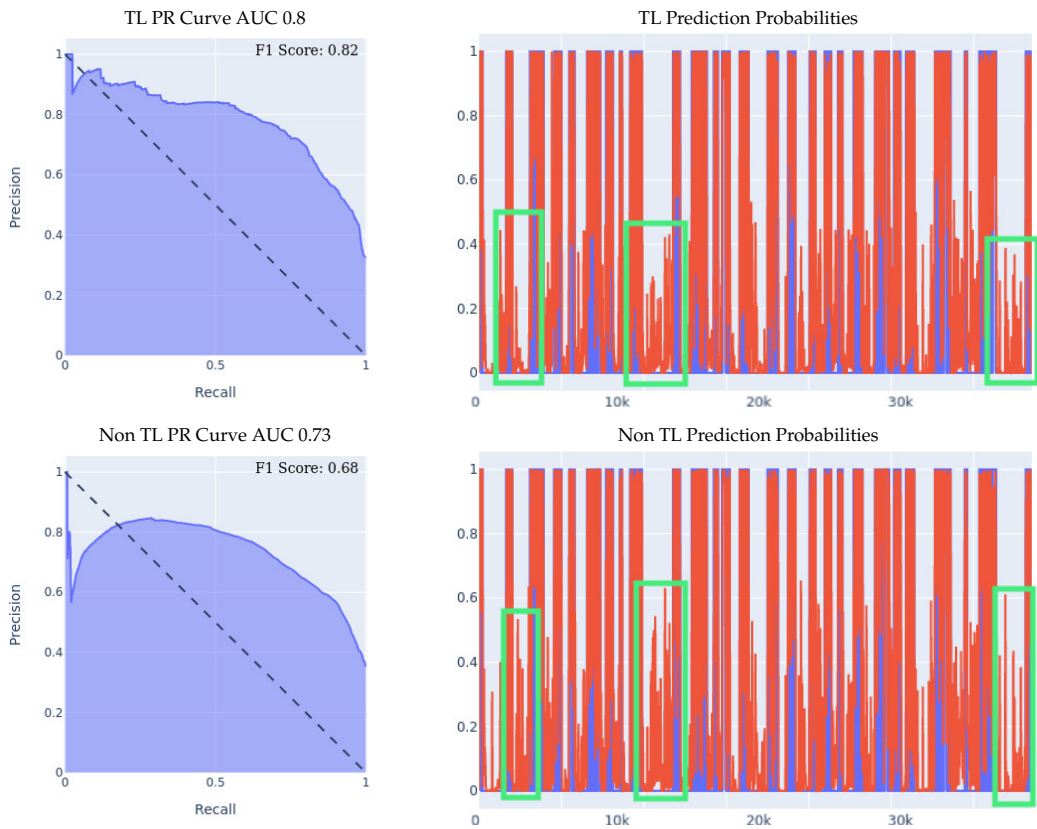


Figure 9. 70/30 Train/Test Data Split Experiment for MSBAND to Huawei. For prediction probabilities, x axis is the time, y axis is the prediction threshold, blue data is the real labels, red data is the prediction probabilities

560 2. **MSBAND to Huawei Experiment II:** the results of the leave-one-person-out cross validation
 561 experiment are presented in Figure 10. If we look at the prediction probabilities plot, we can see
 562 that the transfer learning model has fewer false positive classification instances, for example,
 563 from 8k onwards, we can see that the transfer learning model has no false positive predictions,
 564 while the non-transfer learning model has 2 false positives, and even though on the entries from
 565 2k to 4k on the x axis, both classifiers have 2 false positive classifications, the transfer learning
 566 classifier's prediction threshold value (the red line) only starts spiking prior to the fall close
 567 to entry 4000, in a sense capturing the pre-fall concept, while the non-transfer learning model
 568 spikes all through the non-fall range. Finally, If we look at the F1 Scores, we can see that the
 569 transfer learning model achieved an F1 score that is higher by 10% than the non transfer learning
 570 model as shown in Table 5.
 571 3. **MSBAND to Huawei real-time experiment:** in this experiment, we present the results of
 572 real-time predictions of the transfer learning model against the trained-from-scratch model on
 573 a dataset collected via user feedback by a lab volunteer. The dataset contains 25 falls, and a
 574 series of ADL tasks. The results of the experiment are presented in Figure 11. The transfer
 575 learning model achieves a slightly better PR Curve with a slightly higher AUC. If we look at the
 576 prediction probabilities plot, we can see that the transfer learning predictions overall are less
 577 aggressive, which results in predicting much less false positives as seen at entries 13k onwards,
 578 however, we can also see that the non-transfer learning model's aggressiveness actually makes
 579 it cover true positives (specifically in ranges 5k-7k and 9k-12k) very slightly better than the
 580 transfer learning model, resulting in an F1 score gap of 8% in favor of the transfer learning
 581 model as shown in Table 5.

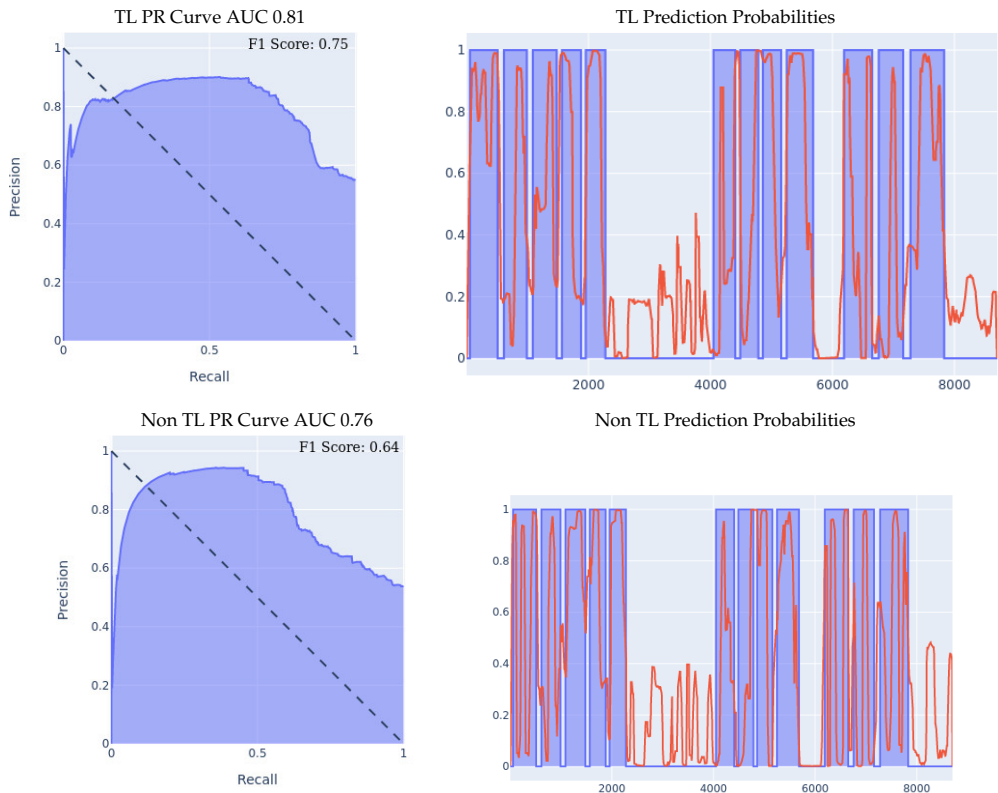


Figure 10. Leave-One-Person-Out Data Split Experiment for MSBAND to Huawei. The averaged F1 score of all the 11 iterations of the cross validation is shown in the top right corner of the PR curve

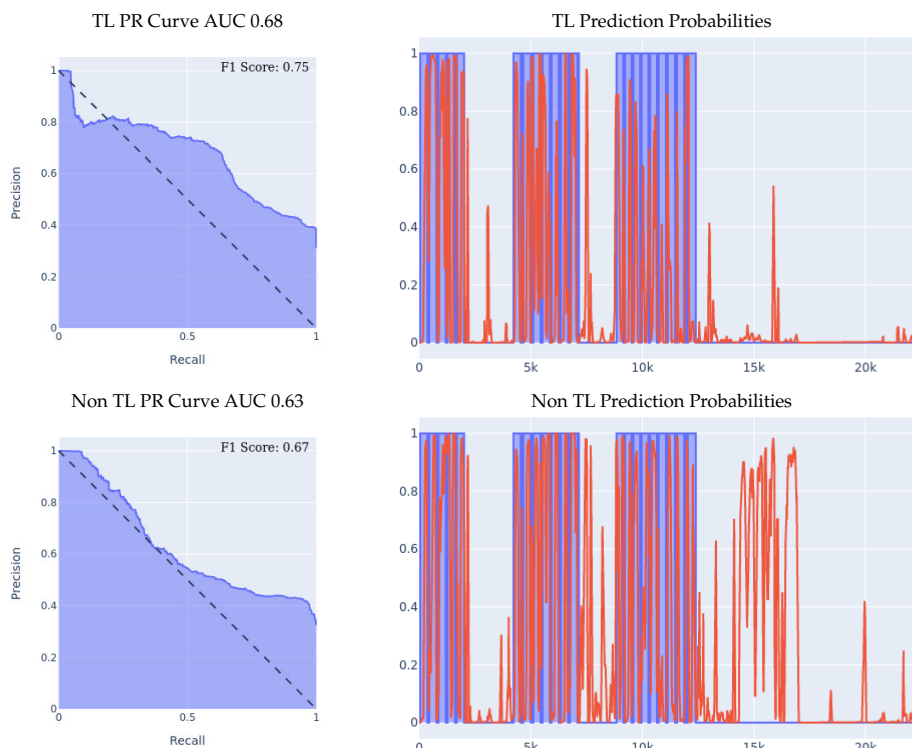


Figure 11. Real-life test experiment. For prediction probabilities, x axis is the time, y axis is the prediction threshold, blue data is the real labels, red data is the prediction probabilities.

582 5.3. Combined Left and Right Wrist Transfer Learning

583 In our third set of experiments, we wanted to test out the effect of using both left wrist and right
584 wrist fall detection models at the same time (meaning that a user would be wearing a wearable device
585 on both wrists), as well as the effect of transfer learning has on that experiment. For our base model,
586 once again, we use the model created by training on the MSBAND dataset, for the same reasons
587 described above. The experiment we conducted in this was was only the leave-one-person-out
588 experiment. We did so because for the 70/30 Train/Test data split experiment, we already managed
589 to get a very good F1 score (as well as good performance in the other metrics) using only one of the
590 wrists, up to 93% in the best case as shown in Table 5.

591 As before, we split the data such that for each cross-validation iteration, we train 2 ensemble
592 classifiers, one of them being the ensemble comprised from the left and right wrist Meta Sensor
593 models which train from scratch on 7 people's data, and the second model being the ensemble
594 comprised from the left and right wrist Meta Sensor models which train on 7 people's data while
595 having the MSBAND classifier as the base model for both members of the ensemble, and then, we
596 evaluate both ensembles' performance on the 8th person's dataset. It is important to note that each
597 member of the ensemble for both classifiers trains only on data specific to its wrist, and that both the
598 training and test dataset are synchronized in time between the left and right wrist, as if a person is
599 wearing two Meta Sensor devices, one on each wrist, and testing the ensemble's fall detection (data
600 was indeed collected by subjects who wore the Meta Sensor devices on both wrists at the same time).

601 We compare the results of the two ensembles as shown in Figure 12. The PR Curve and Prediction
602 plots are taken from a random iteration of the cross validation process, and are representative of the
603 average iteration. We can see the effectiveness of using an ensemble left and right wrist model over
604 a single wrist model, as well as seeing the effectiveness of transfer learning over building a model
605 from scratch throughout all 3 presented metrics. If we look at the PR curve, we can see that the
606 transfer learning model's PR curve is more complete and covers more area resulting in a higher AUC
607 than the normal model. If we also compare both models' PR curves to the leave-one-person-out
608 experiments detailed in sections 5.1 and 5.2, we can see the both models perform better than either
609 of their single wrist counterparts, by having a more complete AUC that covers more area. If we look
610 at the prediction probabilities plot, we can see that the transfer learning ensemble covers more true
611 positives than the ensemble built from scratch (keep in mind that the prediction threshold for a fall
612 is 0.4) while also classifying one less false positive instance. Finally, If we look at the F1 scores, we
613 can see that the transfer learning model achieved an averaged F1 score that is higher by over 7% than
614 the non transfer learning model, and both of them achieved a higher F1 score than either of their one
615 wrist counterparts as shown in Table 5. All those experiments results demonstrated the effectiveness
616 of ensemble models using both left and right wrist wearable accelerometers, achieving the best results
617 out of all the models. Such improvements indicated that we can enhance the fall detection prediction
618 by adding more sensors in a scalable way instead of recollecting and re-training a new set of dataset
619 with all the existing sensors.

620 6. Conclusion and Future Work

621 We presented an approach for fall detection based only on the acceleration data coming from an
622 off-the-shelf wearable edge-device on the wrist of the subject. Fall detection using acceleration data
623 coming strictly from a wearable on the wrist is challenging for the reason that there is a lot of room
624 for false positives, as many activities of daily living (ADL) produce acceleration spikes similar to
625 those of a fall. We collected and presented 3 different types of wearable wrist accelerometers, i.e., the
626 MSBAND smartwatch, the Meta Sensor device, and the Huawei smartwatch. Each device has its own
627 hardware specifications, hence making acceleration datasets produced from these 3 devices differ in
628 many aspects, such as sampling frequency, acceleration unit, axis orientation, etc. Not only are the
629 differences in data between devices a problem, but also, fall data in general is very scarce, as it is very
630 time consuming to collect, leaving us with small datasets across different hardware accelerometers.

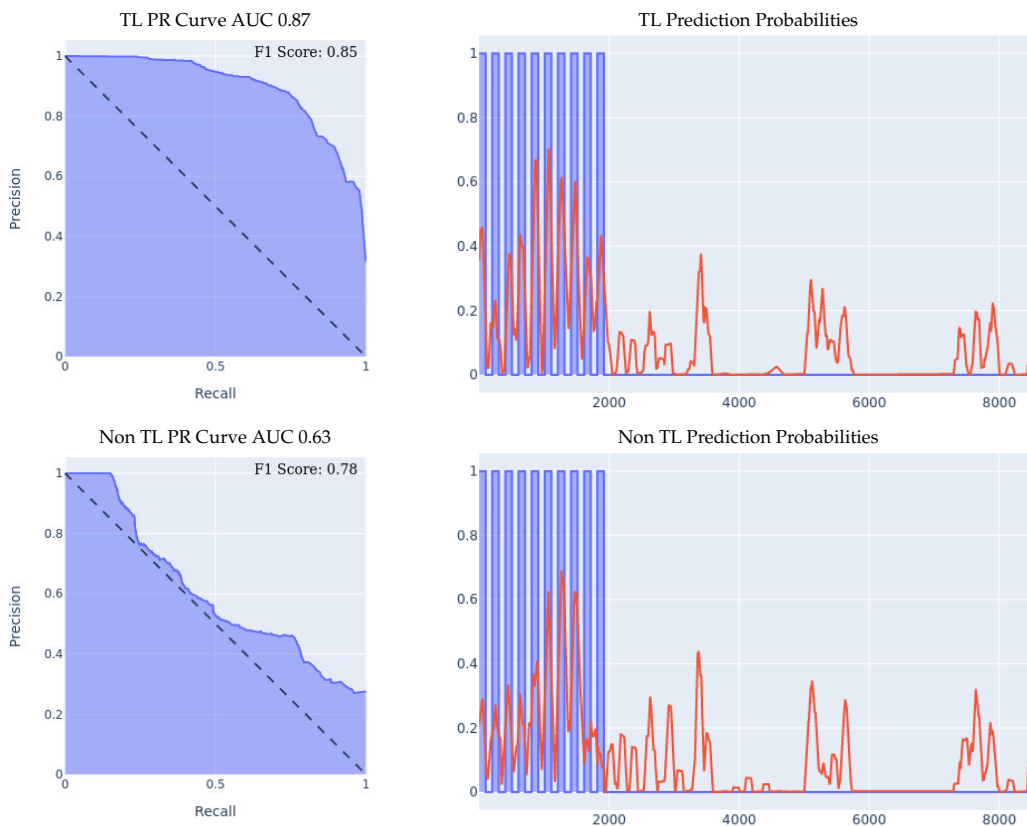


Figure 12. Leave-One-Person-Out Data Split Experiment for ensemble models. For prediction probabilities, x axis is the time, y axis is the prediction threshold, blue data is the real labels, red data is the prediction probabilities. For the F1 Scores, the averaged F1 score of all the 8 iterations of the cross validation is shown in the top right corner of the PR curve

Table 5. Summarization results of F1 score for all experiments. Train/Test denotes the train/test dataset split ratio. A check mark \checkmark represents the transfer learning strategy is applied and a \times denotes the transfer learning is not applied.

Experiment	Transfer Learning	Dataset split strategy	F1 score (%)
Meta Sensor Experiment I	\checkmark	Train/Test: 70/30	0.92
	\times		0.86
Meta Sensor Experiment II	\checkmark	cross validation	0.73
	\times		0.63
MSBAND to Meta Sensor Experiment I	\checkmark	Train/Test: 70/30	0.93
	\times		0.81
MSBAND to Meta Sensor Experiment II	\checkmark	cross validation	0.79
	\times		0.65
MSBAND to Huawei Experiment I	\checkmark	Train/Test: 70/30	0.82
	\times		0.68
MSBAND to Huawei Experiment II	\checkmark	cross validation	0.75
	\times		0.64
MSBAND to Huawei real-time experiment	\checkmark	100% Test	0.75
	\times		0.67
Combined Left and Right wrist experiment	\checkmark	cross validation	0.85
	\times		0.78

631 In order to overcome the problems detailed above and build a model that is robust to dataset size
632 as well as changes in hardware specifications, we experimented with a transfer learning approach,
633 where we would train a base model from scratch using one device's dataset, and then use the trained
634 model as a basis for training a new model on a different device's dataset. Specifically, to solve the
635 target dataset's task, we would not start training from scratch on the target dataset, but use a model
636 which has already been trained on a source dataset of a similar (but not identical) feature space to the
637 target data set, and then, by training that model on the target dataset and having its weights adapt to
638 the target dataset, we would have effectively transferred the source dataset's knowledge to the target
639 dataset's model. We summarized the F-1 score of all the experiments in Table 5.

640 Indeed, we found out through our experiments, that building a model using transfer learning
641 between different wearable devices produces better results than collecting a new set of data using
642 the device and training a model from scratch, as the former model out-performed the latter in all
643 of the experiments we conducted in the paper. We also experimented with building an ensemble
644 fall detection model using both left and right wrist wearable accelerometers, both from scratch and
645 through transfer learning, and found that both ensemble models out-performed their single wrist
646 counterparts, with the transfer learning ensemble model achieving the best results out of all the
647 models. This is encouraging as we can improve the fall detection by adding more sensors in a scalable
648 way. There is no need to re-collect a new set of dataset with all the existing sensors and re-train
649 everything from scratch when a new sensor is added. We just need to collect a small amount of data
650 using the new sensor and leverage a pretrained model with transfer learning to generalize to the
651 newly sensed data. We can then combine the final prediction using an ensemble approach.

652 We have not validated our approach with a target population of different ages, heights, weights,
653 and health conditions. This is a limitation of our current experiment. It is our long-term goal to use
654 part of our funding to recruit older adults for the collection of a small amount of ADL data and use
655 transfer learning for the personalization of fall detection to each person.

656 One immediate direction for future work is the use of [data augmentation method](#), for further
657 solving the small training dataset problem. [Data augmentation](#) method is a process of artificially
658 [increasing the amount of data by generating new data points from existing data that does not](#)
659 [require substantial training data, including Synthetic Minority Oversampling Technique \(SMOTE\)](#)
660 [\[42\]](#), [Transformers](#) [43], [Auto-Encoder](#) [44], [Generative Adversarial Network \(GAN\)](#) [45]. We have
661 started experimentation with GAN for time series data in [46]. Recently, we have also used a GAN
662 product from [Gretel \(Gretel.ai\)](#) to generate synthetic data. Much more research is needed in this area.

663 Our second direction is the use of the transfer learning framework for the purpose of
664 personalization for new edge users, as the transfer learning model personalized very well in the
665 70%/30% Train/Test split experiments. The personalization process can be done by having a
666 pretrained global model that constantly keeps getting re-trained with newly collected data, and
667 whenever a new user is introduced, we collect a small dataset for that user, and train a personalized
668 model specifically for that user through transfer learning from the global model onto the newly
669 collected small dataset.

670 Finally, we also intend to explore other models, for further improving the accuracy performance
671 of fall detection. Currently, there are many time-series prediction models, such as [neural ODEs](#) [47],
672 [CT-RNN](#) [48], [Phased LSTM](#) [49] and [Transformer](#) [50]. We have just started exploring the transformer
673 model.

674 Acknowledgement

675 We thank the National Science Foundation for providing funding under the NSF-SCH grant
676 (2123749) and the NSF Research Experiences for Undergraduates Program (2149950) to perform this
677 piece of work. We thank Colin Campbell for the implementation of the activity labelling App on both
678 watch and phone for data collection process. We thank Ian Martinez Roquebert and Allison Anson
679 for the initial implementation of the LSTM model and transfer learning. We want to thank Awatif

680 Yasmin for conducting the real-time test of the SmartFall system. Finally, we also want to thank 2022
681 REU students Jessica Wang and Elizabeth Kam for manual labelling of the Meta Sensor data.

682 Bibliography

- 683 1. Falls are the leading cause of death in older Americans. <https://www.cdc.gov/media/releases/2016/p0922-older-adult-falls.html>. Accessed: 2019-6-17.
- 684 2. Facts About Falls. <https://www.cdc.gov/falls/facts.html>. Accessed: 2019-6-17.
- 685 3. 2017 Profile of Older Americans. <https://acl.gov/sites/default/files/AgingandDisabilityinAmerica/2017OlderAmericansProfile.pdf>. Accessed: 2019-9-7.
- 686 4. Preventing Falls in Hospitals. <https://www.ahrq.gov/professionals/systems/hospital/fallpxtoolkit/index.html>. Accessed: 2019-11-18.
- 687 5. Tacconi, C.; Mellone, S.; Chiari, L. Smartphone-based applications for investigating falls and mobility. 2011 5th International Conference on Pervasive Computing Technologies for Healthcare (PervasiveHealth) and Workshops, 2011, pp. 258–261.
- 688 6. Chen, L.; Li, R.; Zhang, H.; Tian, L.; Chen, N. Intelligent fall detection method based on accelerometer data from a wrist-worn smart watch. *Measurement* **2019**, *140*, 215 – 226.
- 689 7. Medical Life Alert Systems. <http://www.lifealert.com>.
- 690 8. Mobilehelp Smart. <https://www.mobilehelp.com/pages/smart>. Accessed: 2019-11-18.
- 691 9. Apple Watch Series 4. <http://www.apple.com/apple-watch-series-4/activity/>. Accessed: 2019-04-18.
- 692 10. RightMinder - Fall Detection for Android Smartwatches and Android Phones. <https://mhealthspot.com/2017/03/rightminder-android-wear-app-seniors/>. Accessed: 2022-12-14.
- 693 11. Mauldin, T.R.; Ngu, A.H.; Metsis, V.; Canby, M.E. Ensemble Deep Learning on Wearables Using Small Datasets. *ACM Trans. Comput. Healthcare* **2021**, *2*.
- 694 12. Mauldin, T.R.; Canby, M.E.; Metsis, V.; Ngu, A.H.; Rivera, C.C. SmartFall: A Smartwatch-Based Fall Detection System Using Deep Learning. *Sensors* **2018**, *18*.
- 695 13. Seraji-Bzorgzad, N.; Paulson, H.; Heidebrink, J. Neurologic examination in the elderly. *Handbook of clinical neurology* **2019**, *167*, 73–88.
- 696 14. Vaswani, A.; Shazeer, N.; Parmar, N.; Uszkoreit, J.; Jones, L.; Gomez, A.N.; Kaiser, L.; Polosukhin, I. Attention is all you need. *Advances in neural information processing systems* **2017**, *30*.
- 697 15. Krizhevsky, A.; Sutskever, I.; Hinton, G.E. Imagenet classification with deep convolutional neural networks. *Communications of the ACM* **2017**, *60*, 84–90.
- 698 16. Bahdanau, D.; Chorowski, J.; Serdyuk, D.; Brakel, P.; Bengio, Y. End-to-end attention-based large vocabulary speech recognition. 2016 IEEE international conference on acoustics, speech and signal processing (ICASSP). IEEE, 2016, pp. 4945–4949.
- 699 17. Zhu, X.J. Semi-supervised learning literature survey **2005**.
- 700 18. Zhuang, F.; Qi, Z.; Duan, K.; Xi, D.; Zhu, Y.; Zhu, H.; Xiong, H.; He, Q. A comprehensive survey on transfer learning. *Proceedings of the IEEE* **2020**, *109*, 43–76.
- 701 19. Weiss, K.; Khoshgoftaar, T.M.; Wang, D. A survey of transfer learning. *Journal of Big data* **2016**, *3*, 1–40.
- 702 20. Maqsood, M.; Nazir, F.; Khan, U.; Aadil, F.; Jamal, H.; Mehmood, I.; Song, O.y. Transfer learning assisted classification and detection of Alzheimer’s disease stages using 3D MRI scans. *Sensors* **2019**, *19*, 2645.
- 703 21. Shin, H.C.; Roth, H.R.; Gao, M.; Lu, L.; Xu, Z.; Nogues, I.; Yao, J.; Mollura, D.; Summers, R.M. Deep convolutional neural networks for computer-aided detection: CNN architectures, dataset characteristics and transfer learning. *IEEE transactions on medical imaging* **2016**, *35*, 1285–1298.
- 704 22. Byra, M.; Wu, M.; Zhang, X.; Jang, H.; Ma, Y.J.; Chang, E.Y.; Shah, S.; Du, J. Knee menisci segmentation and relaxometry of 3D ultrashort echo time cones MR imaging using attention U-Net with transfer learning. *Magnetic resonance in medicine* **2020**, *83*, 1109–1122.
- 705 23. Tang, X.; Du, B.; Huang, J.; Wang, Z.; Zhang, L. On combining active and transfer learning for medical data classification. *IET Computer Vision* **2019**, *13*, 194–205.
- 706 24. Zeng, M.; Li, M.; Fei, Z.; Yu, Y.; Pan, Y.; Wang, J. Automatic ICD-9 coding via deep transfer learning. *Neurocomputing* **2019**, *324*, 43–50.
- 707 25. Krizhevsky, A.; Sutskever, I.; Hinton, G.E. Imagenet classification with deep convolutional neural networks. *Advances in neural information processing systems*, 2012, pp. 1097–1105.

731 26. Deng, J.; Dong, W.; Socher, R.; Li, L.J.; Li, K.; Fei-Fei, L. Imagenet: A large-scale hierarchical image
732 database. 2009 IEEE conference on computer vision and pattern recognition. Ieee, 2009, pp. 248–255.

733 27. Marcus, D.S.; Fotenos, A.F.; Csernansky, J.G.; Morris, J.C.; Buckner, R.L. Open access series of imaging
734 studies: longitudinal MRI data in nondemented and demented older adults. *Journal of cognitive
735 neuroscience* **2010**, *22*, 2677–2684.

736 28. Donahue, J.; Jia, Y.; Vinyals, O.; Hoffman, J.; Zhang, N.; Tzeng, E.; Darrell, T. Decaf: A deep convolutional
737 activation feature for generic visual recognition. International conference on machine learning. PMLR,
738 2014, pp. 647–655.

739 29. Palanisamy, K.; Singhania, D.; Yao, A. Rethinking CNN models for audio classification. *arXiv preprint
740 arXiv:2007.11154* **2020**.

741 30. Koike, T.; Qian, K.; Kong, Q.; Plumbley, M.D.; Schuller, B.W.; Yamamoto, Y. Audio for audio is better? An
742 investigation on transfer learning models for heart sound classification. 2020 42nd Annual International
743 Conference of the IEEE Engineering in Medicine & Biology Society (EMBC). IEEE, 2020, pp. 74–77.

744 31. Gemmeke, J.F.; Ellis, D.P.; Freedman, D.; Jansen, A.; Lawrence, W.; Moore, R.C.; Plakal, M.; Ritter, M.
745 Audio set: An ontology and human-labeled dataset for audio events. 2017 IEEE international conference
746 on acoustics, speech and signal processing (ICASSP). IEEE, 2017, pp. 776–780.

747 32. Ni, J.; Sarbajna, R.; Liu, Y.; Ngu, A.H.; Yan, Y. Cross-modal knowledge distillation for Vision-to-Sensor
748 action recognition. ICASSP 2022-2022 IEEE International Conference on Acoustics, Speech and Signal
749 Processing (ICASSP). IEEE, 2022, pp. 4448–4452.

750 33. Ni, J.; Ngu, A.H.; Yan, Y. Progressive Cross-modal Knowledge Distillation for Human Action Recognition.
751 Proceedings of the 30th ACM International Conference on Multimedia, 2022, pp. 5903–5912.

752 34. Li, F.; Shirahama, K.; Nisar, M.A.; Huang, X.; Grzegorzek, M. Deep Transfer Learning for Time Series
753 Data Based on Sensor Modality Classification. *Sensors* **2020**, *20*.

754 35. Fawaz, H.I.; Forestier, G.; Weber, J.; Idoumghar, L.; Muller, P.A. Deep learning for time series classification:
755 a review. *Data Mining and Knowledge Discovery* **2019**, *33*, 917–963.

756 36. Gikunda, P.; Jouandeau, N. Homogeneous Transfer Active Learning for Time Series Classification. 2021
757 20th IEEE International Conference on Machine Learning and Applications (ICMLA), 2021, pp. 778–784.

758 37. Morales, F.J.O.n.; Roggen, D. Deep Convolutional Feature Transfer across Mobile Activity Recognition
759 Domains, Sensor Modalities and Locations; Association for Computing Machinery: New York, NY, USA,
760 2016.

761 38. Zhou, X.; Zhai, N.; Li, S.; Shi, H. Time Series Prediction Method of Industrial Process with Limited Data
762 Based on Transfer Learning. *IEEE Transactions on Industrial Informatics* **2022**, pp. 1–10.

763 39. Villar, J.R.; de la Cal, E.; Fañez, M.; González, V.M.; Sedano, J. User-centered fall detection using
764 supervised, on-line learning and transfer learning. *Progress in Artificial Intelligence* **2019**, *8*, 453–474.

765 40. Ngu, A.H.; Gutierrez, M.; Metsis, V.; Nepal, S.; Sheng, Q.Z. IoT Middleware: A Survey on Issues and
766 Enabling Technologies. *IEEE Internet of Things Journal* **2017**, *4*, 1–20.

767 41. Ngu, A.H.H.; Eyyitayo, J.S.; Yang, G.; Campbell, C.; Sheng, Q.Z.; Ni, J. An IoT Edge Computing Framework
768 Using Cordova Accessor Host. *IEEE Internet of Things Journal* **2022**, *9*, 671–683.

769 42. Chawla, N.V.; Bowyer, K.W.; Hall, L.O.; Kegelmeyer, W.P. SMOTE: synthetic minority over-sampling
770 technique. *Journal of artificial intelligence research* **2002**, *16*, 321–357.

771 43. Kumar, V.; Choudhary, A.; Cho, E. Data augmentation using pre-trained transformer models. *arXiv
772 preprint arXiv:2003.02245* **2020**.

773 44. Kuroyanagi, I.; Hayashi, T.; Adachi, Y.; Yoshimura, T.; Takeda, K.; Toda, T. Anomalous sound detection
774 with ensemble of autoencoder and binary classification approaches. Technical report, DCASE2021
775 Challenge, Tech. Rep, 2021.

776 45. Mariani, G.; Scheidegger, F.; Istrate, R.; Bekas, C.; Malossi, C. Bagan: Data augmentation with balancing
777 gan. *arXiv preprint arXiv:1803.09655* **2018**.

778 46. Li, X.; Metsis, V.; Wang, H.; Ngu, A. *TTS-GAN: A Transformer-Based Time-Series Generative Adversarial
779 Network*; Vol. 13263 LNAI, *Lecture Notes in Computer Science*, Springer Science and Business Media
780 Deutschland GmbH: Texas State University, 2022.

781 47. Kidger, P.; Morrill, J.; Foster, J.; Lyons, T. Neural controlled differential equations for irregular time series.
782 *Advances in Neural Information Processing Systems* **2020**, *33*, 6696–6707.

783 48. Hasani, R.; Lechner, M.; Amini, A.; Rus, D.; Grosu, R. Liquid time-constant networks. Proceedings of the
784 AAAI Conference on Artificial Intelligence, 2021, Vol. 35, pp. 7657–7666.

785 49. Liu, Y.; Gong, C.; Yang, L.; Chen, Y. DSTP-RNN: A dual-stage two-phase attention-based recurrent neural
786 network for long-term and multivariate time series prediction. *Expert Systems with Applications* **2020**,
787 143, 113082.

788 50. Li, S.; Jin, X.; Xuan, Y.; Zhou, X.; Chen, W.; Wang, Y.X.; Yan, X. Enhancing the locality and breaking the
789 memory bottleneck of transformer on time series forecasting. *Advances in neural information processing
790 systems* **2019**, 32.

791 © 2023 by the author. Submitted to *Sensors* for possible open access publication under the terms and conditions
792 of the Creative Commons Attribution license (<http://creativecommons.org/licenses/by/4.0/>)